

# Biomechanical optimisation strategy for selecting native shrubs and herbaceous plants with superior soil and water conservation properties in combating land degradation in central-western Inner Mongolia

RILE GE\*, WEI ZHAO†, HUI ZHI, YAHUI LU, SHUAIXIN WEI

College of Desert Control Science and Engineering, Inner Mongolia Agricultural University, Hohhot, China

\*Corresponding author: gerile197081@126.com

†Joint first author

**Citation:** Ge R., Zhao W., Hui Z., Yahui L., Shuaixin W. (2026): Biomechanical optimisation strategy for selecting native shrubs and herbaceous plants with superior soil and water conservation properties in combating land degradation in central-western Inner Mongolia. *J. For. Sci.*, 72: 42–55.

**Abstract:** To enhance the biomechanical database of plant root systems for soil reinforcement and erosion control in arid and semi-arid regions, and to provide a scientific basis for selecting superior native shrub and herb species in forestry and grassland measures for desertification control in central and western Inner Mongolia, this study investigated the root-soil interfacial friction characteristics of five typical native plant species – *Caragana korshinskii* and *Hippophae rhamnoides*, the semi-shrub *Hedysarum mongolicum*, and the perennial herbs *Medicago sativa* and *Astragalus adsurgens* – in two widely distributed non-zonal soils: loessial soil and aeolian sandy soil. Single-root pull-out tests were conducted on indoor-prepared root-soil composite samples to examine their responses to varying soil moisture levels. The results showed that within a soil moisture range of 4.6% to 20.6%, the single-root pull-out resistance and shear strength of all five species in both soil types followed a quadratic model  $Y = ax^2 + bx + c$  (with all multiple correlation coefficients  $> 0.5$ ), initially increasing and then decreasing with rising moisture content. Peak values occurred at 8.6% moisture, with consistently higher values observed in loessial soil than in aeolian sandy soil. This indicates an optimal soil moisture level for maximising root-soil interfacial friction resistance. Among the species, *Hippophae rhamnoides* and *Medicago sativa* exhibited superior pull-out performance in both soils, with *Hippophae rhamnoides* showing greater sensitivity to environmental variations in loessial soil. Redundancy analysis identified soil type and moisture content as key factors explaining variations in root pull-out shear strength. These findings demonstrate that mixed-species plantations, leveraging complementary root traits, can form more complex and stable root-soil structures, thereby enhancing surface soil mechanical stability. Further research is needed to elucidate the adaptive mechanisms linking plant traits, environmental conditions, and biomechanical characteristics.

**Keywords:** pullout resistive strength; root-soil interface; single resistance pull; soil moisture content

---

Supported by the Research Program of the Inner Mongolia Autonomous Region Education Department on 'Strengthening the Construction of China's Northern Important Ecological Security Barrier': Study on the Key Mechanisms for Improving Quality and Efficiency of Ecological Shelterbelt Seabuckthorn Plantations in the Pisha Sandstone Area of the Yellow River Basin in Inner Mongolia (STAQZX202309); the Inner Mongolia Natural Science Foundation Project 'Response Mechanism of Soil Reinforcement and Anti-erosion by Seabuckthorn Roots to Pruning and Rejuvenation' (2021MS04011); the National Natural Science Foundation of China Project 'Biomechanical Response Mechanism of Plant Root Self-repair after Soil Reinforcement and Anti-erosion Damage under Gradient Stress' (41867011); and the Special Project of the 14<sup>th</sup> Five-Year Plan for Educational Science Research in Inner Mongolia Autonomous Region (2023NGHZX-LD165).

© The authors. This work is licensed under a Creative Commons Attribution-NonCommercial 4.0 International (CC BY-NC 4.0).

China is one of the countries facing severe soil and water erosion globally. Serious soil erosion leads to decreased soil fertility, increased droughts and floods, ecosystem imbalance, significant damage to human settlements, and constraints on sustainable regional economic development (Berry, Roderick 2005). In recent years, China has actively promoted ecological civilisation construction, identified soil and water conservation as a key strategic task, and achieved remarkable results in soil erosion control. Nevertheless, the situation of soil and water erosion across the country remains challenging, with western regions being particularly affected. Restricted by adverse natural conditions such as drought, limited rainfall, and poor soil fertility, the restoration of forest and grassland vegetation is challenging. At the same time, irrational human economic activities, particularly land excavation and subsidence caused by mining, severely damage native vegetation and further exacerbate the deterioration of the regional ecological environment (Bardgett et al. 2014). Among soil and water conservation measures, biological forestry and grass measures are the most proactive and effective approaches. They not only help reduce soil erosion but also entail low economic costs and can contribute to improving the local microclimate (Hales et al. 2013). In slope protection engineering, the soil-reinforcing effect of plant roots is achieved through the synergistic action of taproots and fibrous roots. Fibrous and shallow fine roots, due to their extensive distribution, primarily function as reinforcement, while taproots and thick roots, with their high bending strength and deeper penetration, mainly provide anchorage and support (Zhang et al. 2020). Furthermore, plant roots absorb soil moisture, thereby reducing pore water pressure within the slope, enhancing the stability of the surface soil, and significantly lowering the probability of geological hazards such as landslides. Within the soil, the intricate network of plant roots intertwines with the soil to form a root-soil composite. In this composite system, roots enhance soil cohesion through mechanical actions such as oblique tension and vertical anchorage, significantly strengthening the strength of the root-permeated soil layer. Since the deformation modulus of plant roots is generally higher than that of the soil matrix, when relative displacement tends to occur or actually occurs at the root-soil interface, the interfacial frictional

resistance can convert the sliding force into tensile stress within the roots. This effectively restrains soil deformation and enhances its ductility. Under vertical pressure, root-free soil is prone to vertical compression and lateral deformation. In contrast, rooted soil exhibits significantly reduced lateral deformation due to the frictional interaction between the roots and the soil. This frictional effect not only improves the shear strength of the soil but also suppresses its lateral expansion. By increasing confining pressure and reducing shear stress, it enhances the overall stability of the soil mass (Tosi 2007). In other words, the frictional characteristics at the root-soil interface play a significant role in the internal stability of the root-soil composite.

The reinforcement theory and the anchorage theory are currently the two widely recognised mechanical mechanisms by which plant roots stabilise soil. The absorption of water and nutrients by plant roots, combined with their anchoring effect in the soil, meets the needs for stable plant growth. In soil erosion-prone areas, the composite formed by roots and soil significantly improves the soil's mechanical properties, enhances its erosion resistance, and increases slope stability (Flores-Rentería et al. 2018). Regarding the frictional characteristics at the root-soil interface, scholars domestically and internationally have conducted relevant research and achieved corresponding results, primarily manifested in aspects such as the root-soil interface friction mechanism, differences in frictional characteristics among different plant species, and influencing factors. Currently, many experts and scholars both domestically and internationally have conducted research on the mechanical roles and characteristics of plant roots in soil stabilisation, erosion resistance, and the prevention of soil erosion. These studies encompass areas such as the ultimate tensile force and tensile strength of plant roots (Campbell, Hawkins 2003), the shear resistance characteristics of root-soil composites (Bordoni et al. 2016), and the frictional properties at the root-soil interface (Genet et al. 2005). These aspects represent the primary mechanical factors influencing the soil-stabilising and erosion-resistant functions of root systems. Plant roots are in close contact with the soil, and the interplay of various factors results in the root-soil interface exhibiting complex and variable frictional characteristics. Schwarz et al. (2010) investigated the effects of soil particle size and moisture con-

tent on the friction between roots and soil. The results indicated that the magnitude of the maximum root pull-out resistance (1–5 kPa) has a significant influence on slope stability. The research results of Ji et al. (2018) showed that when the loading rate increased from  $10 \text{ mm} \cdot \text{min}^{-1}$  to  $300 \text{ mm} \cdot \text{min}^{-1}$ , the maximum pull-out force increased by 10% to 15%. Gonzalez-Ollauri and Mickovski (2017) indicated that there exists a specific soil moisture content at which the reinforcing effect of plant roots on the soil is optimised.

In summary, differences in biological characteristics among plant species and site conditions lead to variations in the biomechanical properties of root systems, which in turn affect the frictional characteristics at the root-soil interface and ultimately influence soil reinforcement and water retention effectiveness. In light of this, this study focuses on the root systems of five typical native shrubs and grasses in central and western Inner Mongolia – the shrubs *Caragana korshinskii* and *Hippophae rhamnoides*, the semi-shrub *Hedysarum mongolicum*, and the perennial herbs *Medicago sativa* and *Astragalus adsurgens*. Indoor single-root pull-out friction tests were conducted on root-soil composites to investigate the frictional characteristics and their variation patterns at the root-soil interface under different soil moisture levels in two widely distributed typical azonal soils in the region: loessial soil and aeolian sandy soil. The study aims to reveal interspecific differences and common patterns in the biomechanical properties of root-soil systems, thereby contributing to the improvement of the biomechanical database for soil fixation and erosion resistance by plants in arid and semi-arid regions. Furthermore, it provides theoretical guidance for optimising the selection of native shrubs and grasses and their mixed-species configurations in biological and vegetative measures for combating land degradation in central and western Inner Mongolia.

**Overview of the study area.** The sampling site was located at the Heidaigou open-pit coal mine dump site in Jungar Banner, Ordos City, which lies in the semi-arid loess hilly and gully region of Inner Mongolia. Its geographical coordinates range from  $111.22^\circ\text{E}$  to  $111.33^\circ\text{E}$  and  $39.72^\circ\text{N}$  to  $39.82^\circ\text{N}$ , with an elevation between 1 025 m a.s.l. and 1 302 m a.s.l. The mining area is situated in the western part of the Loess Plateau, at the junction of Shanxi, Shaanxi, and Inner Mongolia, covering

a total area of  $52.11 \text{ km}^2$ . The climate is characterised as a mid-temperate semi-arid continental type, with an average annual temperature of approximately  $7.2^\circ\text{C}$  and an average annual precipitation of 404.1 mm. About 70% of the precipitation is concentrated in the rainy season from July to September, featuring short-duration, high-intensity rainfall events. The area is rich in wind energy resources, with a multi-year average wind speed of  $3.6 \text{ m} \cdot \text{s}^{-1}$ , an average of 42.2 days of strong wind per year, and an annual sandstorm frequency ranging from 17 to 26 days. The landform type is typical of loess hilly terrain, characterised by thick loess deposits covering the surface, well-developed gullies, and a dendritic water system formed by main and branch gullies, indicating intense erosion. The geological structure consists of superimposed bedrock strata from the Paleozoic to Mesozoic eras, tertiary cohesive soil, and quaternary loess deposits. The soil types are primarily azonal soils, including loessial soil and aeolian sandy soil, with zonal soil distribution being less distinct. The soil in the artificial dump site at the sampling location is backfill material, which has been compacted by heavy machinery, resulting in high density, low porosity, and poor permeability.

## MATERIAL AND METHODS

**Root and soil investigation.** In mid-August 2024, sample plots were established under identical site conditions on the internal dump platform of the Heidaigou open-pit mine (platform elevation: 1 251 m a.s.l.; central geographic coordinates:  $39.79^\circ\text{N}$ ,  $111.27^\circ\text{E}$ ). The study targeted five species of 3-year-old shrubs and herbs: *Caragana korshinskii*, *Hippophae rhamnoides*, *Hedysarum mongolicum*, *Medicago sativa*, and *Astragalus adsurgens*. The size of each sample plot was determined based on the plant life form and planting density. For the two shrub species, *Hippophae rhamnoides* and *Caragana korshinskii*, which were established by seedling planting, the plot size was set at  $50 \times 50 \text{ m}$ , with a spacing of  $1.5 \times 2 \text{ m}$ . Three replicate plots were established for each species. For the semi-shrub *Hedysarum mongolicum* and the two herbaceous species, which were established by direct seeding with a coverage of 60%, the plot size was set at  $10 \times 10 \text{ m}$ , also with three replicates per species. Within each plant sample plot, 30 individuals were randomly selected to measure

their plant height, crown width, and ground diameter. The average values for these growth indicators were calculated for each species across the three sample plots. The mean of these averages was then computed to represent the overall average for each plant species. From the three replicate plots of each species, 3 to 5 individuals whose growth indicators were closest to the overall average were selected as standard plants and tagged for further study. Root excavation, collection, and related sampling and measurements were conducted on these standard plants. The growth status of the five plant species and the selection of standard plants are presented in Table 1.

**Excavation and collection of root systems and undisturbed soil samples.** The excavation and collection of root systems were conducted beneath the standard plants of the test species. Root system excavation began at a distance of 1.5–2.0 m from one side of the standard plant. Using the contraction method, the roots were carefully excavated sequentially from the outside inward, ensuring the integrity of the root system as much as possible. Roots within the required diameter range were collected, placed in black plastic bags, and misted with water to prevent dehydration. After collection, the samples were promptly transported to the laboratory and stored in a constant-temperature chamber at 4 °C to ensure the experiments were completed as quickly as possible. For the loessial soil, three soil profiles were excavated from a relatively flat, unclaimed area under the same site conditions as the platform of the internal waste dump at the sampling site. Each profile had a depth of 100 cm, and samples were taken at 20 cm intervals. In each layer, three undisturbed soil cores were collected using a cutting ring with a diameter of 50.46 mm and a height of 50 mm, arranged in a triangular pattern. A total of 15 soil samples were taken from each profile, resulting in 45 samples, which were sealed

in aluminium boxes. Additionally, 5–7 kg of soil was collected as experimental soil and brought back to the laboratory. The aeolian sandy soil was collected from the nearby moving sand dunes of the Kubuqi Desert. The soil sampling method was consistent with the aforementioned approach and is not repeated here.

**Selection of experimental roots.** The study on the root-soil interface friction characteristics of five plant species under two soil types and five different soil moisture gradients focused on their representative roots. Research on these representative roots has been published separately by the research team (Fan, Chen 2010; Docker, Hubble 2008; Noorasyikin et al. 2022). The findings on representative roots indicated that for *Caragana korshinskii*, *Hedysarum mongolicum*, *Medicago sativa*, and *Astragalus adsurgens*, the representative root diameter ranges were 0–0.5 mm, 0.5–1 mm, and 1–1.5 mm, while for *Hippophae rhamnoides*, the representative root diameter ranges were 0.5–1 mm and 1–1.5 mm. This means that for these five plant species, the growth indicators (including root diameter, root length, root surface area, and the percentage of root dry weight to total roots) of roots with diameters less than 2 mm were superior to those in other root diameter ranges. In light of this, when conducting single-root tensile pull-out tests under different moisture levels in this study, fine roots within the common representative root diameter range of 1–1.5 mm for the five plant species were selected for comparative research. Additionally, no fewer than 30 valid single-root pull-out tests were conducted for the 1–1.5 mm range, and the average of the data from these 30 valid tests was taken as the value representing that specific soil moisture level.

**Basic physical and geotechnical properties of undisturbed soil.** The moisture content and bulk density of undisturbed soil were determined using

Table 1. Growth performance of five plant species and selection of standard plants

Plant species	Plant height (cm)	Crown width (cm)		Root diameter (maximum) (mm)
		East-West	North-South	
<i>Medicago sativa</i>	64.27 ± 9.68	52.37 ± 12.31	48.47 ± 12.34	3.03 ± 0.56
<i>Caragana Korshinskii</i>	118.23 ± 12.16	72.05 ± 9.18	74.12 ± 10.59	3.98 ± 1.29
<i>Hedysarum mongolicum</i>	105.02 ± 20.32	85.18 ± 27.61	82.90 ± 30.81	1.79 ± 0.12
<i>Hedysarum mongolicum</i>	97.73 ± 17.12	68.23 ± 17.36	66.56 ± 15.32	7.09 ± 2.16
<i>Astragalus adsurgens</i>	67.72 ± 10.28	60.12 ± 11.74	58.36 ± 10.38	2.92 ± 0.13

the ring knife sampling and oven-drying method at 105 °C. For the determination of soil mechanical composition, the collected undisturbed soil was passed through a 2 mm sieve, and an appropriate amount of the sieved soil was subjected to particle size analysis using the Mastersizer 3000 laser particle size analyser (Malvern Panalytical, United Kingdom). The results are shown in Table 2. According to the Kachinsky classification system, the soil textures of the experimental soils are classified as light loam and sand.

The liquid limit and plastic limit tests of the undisturbed soil were conducted in the laboratory using a combined liquid-plastic limit tester. The data obtained was used for a preliminary geotechnical classification of the two experimental soils according to the 'Standard for Engineering Classification of Soil' (GB/T 50145-2007). As shown in Table 2, the fine fraction content of the loessial soil is 54.83%, which is greater than 50% of the total soil mass, thus classifying it as fine-grained soil. Within the fine-grained soil category, if the coarse fraction content is greater than 25% but less than 50% of the total soil mass, it is termed coarse-grained fine-grained soil. The fine fraction content of the aeolian sandy soil is 3.59%, which is less than 5% of the total soil mass, thus classifying it as sand. The liquid limit and plastic limit are two important physical indicators of cohesive soils and can be used to cal-

culate the soil's plasticity index and liquidity index (Ali et al. 2012). Between the two experimental soils, only the loessial soil is fine-grained; therefore, liquid limit and plastic limit tests were conducted only on the loessial soil. The results show a plasticity index  $Ip = 8.62$  (i.e.  $Ip < 10$ ) and a liquid limit  $WL = 27.04\%$  (i.e.  $WL < 50\%$ ). Based on the position of its plasticity index  $Ip$  and liquid limit  $WL$  in the plasticity chart, the loessial soil is classified as sandy low-liquid-limit silt (MLS), while the aeolian sandy soil is classified as sand (S).

**Methods.** Under the conditions of a soil moisture content of 8.6% (measured natural moisture content) and soil dry densities of  $1.59 \text{ g} \cdot \text{cm}^{-3}$  for loessial soil and  $1.48 \text{ g} \cdot \text{cm}^{-3}$  for aeolian sandy soil, straight root segments with diameters of 1–1.5 mm were selected and prepared into 8 cm long segments for testing. Among these, a 2 cm section was clamped by the fixture, while a 6 cm segment was embedded within the test container (PVC pipe) (Figure 1). A TY8000 servo-controlled testing machine (Tian Yuan, China) was used for the pull-out tests. The preparation of root-soil composite specimens under different moisture content levels followed the methods described by Fan et al. (2021), Xing et al. (2023), Fang et al. (2024) and Zhang et al. (2025). The five different soil moisture content gradients were designed to reflect the dynamic variation characteristics of soil moisture in the natural

Table 2. Analysis results table of mechanical composition for the two experimental soils

Soil types	Soil mechanical composition (%)						
	> 2 mm	1–2 mm	0.5–1 mm	0.25–0.5 mm	0.25–0.075 mm	0.005–0.075 mm	< 0.005 mm
Loessial soil	$0.57 \pm 0.04$	$1.51 \pm 0.08$	$8.17 \pm 0.93$	$3.38 \pm 0.25$	$31.54 \pm 2.22$	$53.31 \pm 2.67$	$1.52 \pm 0.027$
Aeolian sandy soil	0	0	$0.2 \pm 0.03$	$4.66 \pm 0.28$	$91.55 \pm 5.95$	$2.5 \pm 0.02$	$1.09 \pm 0.01$

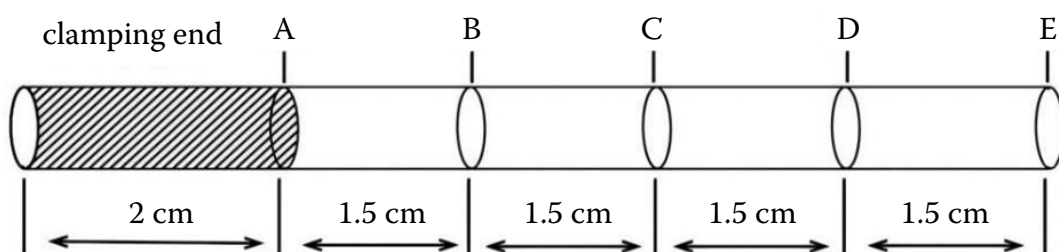


Figure 1. Schematic diagram of test roots

sampling environment. The experimental study was conducted at these five different moisture content levels: 4.60%, 8.60% (the measured natural moisture content of the undisturbed soil), 12.60%, 16.60%, and 20.60% (all below the saturated moisture content of both the loessial soil and aeolian sandy soil).

A PVC pipe with an inner diameter of 6 cm and a length of 11 cm was used, with a symmetrical 1 cm diameter circular hole drilled at its midpoint. One end of the pipe was tightly sealed with a circular wooden disc (1 cm thick). Remoulded soil, prepared and left to stand for 24 h, was added to the pipe. When the soil reached the level of the circular hole, a root was passed through the hole, leaving the clamping end exposed. Soil filling continued until the pipe was full, and another circular wooden disc was placed on top to compact the soil. The wooden disc at the other end was then removed, and additional soil was added. Soil was repeatedly added at both ends of the pipe to ensure the test root remained centred in the circular hole and to avoid friction with the hole edges. When the dry density of the soil in the PVC pipe met the experimental requirements, the prepared specimen was fixed into a custom-made clamp for later use. For the single-root pull-out test, the number of valid repetitions for each soil moisture level was no less than 15. The preparation process of the root-soil composite specimens, soil compaction, and the pull-out test setup are illustrated in Figure 2. After preparation, the specimen clamp was fixed onto the testing machine, and the pull-out speed was set to 150 mm·min<sup>-1</sup>.

Based on the physical properties of the undisturbed soil and the habitat conditions at the sampling site, the moisture content of the remoulded soil was set to the measured natural moisture

content of 8.5%. The calculations for the required amounts of air-dried soil and water to prepare the remoulded soil are shown in Equations (1) and (2). The prepared soil was sealed, protected from light, and allowed to stand for 24 h before use, allowing the properties of the remoulded soil to more closely approximate those of the undisturbed soil.

$$m = (1 + 0.01\omega_0)V\rho_d \quad (1)$$

where:

- $m$  – mass of air-dried soil required (g);
- $\omega_0$  – moisture content of the air-dried soil (%);
- $\rho_d$  – dry density of the experimental soil (g·cm<sup>-3</sup>);
- $V$  – volume of the specimen (cm<sup>3</sup>).

$$m_0 = \frac{1}{1 + 0.01\omega_0} \times (\omega - \omega_0) \quad (2)$$

where:

- $m_0$  – mass of water required for the specimen (g);
- $\omega_0$  – moisture content of the air-dried soil (%);
- $\omega$  – target moisture content to be configured for the soil (%).

The single-root pull-out test for the root-soil composite is based on two assumptions: (i) During the root extraction process, the frictional stress at the root-soil interface is uniformly distributed; (ii) Along the root axis direction, the displacement of the root-soil composite is equivalent to the shear displacement at the root-soil interface. The external force causing this displacement is the pull-out shear force at the root-soil interface, and the maximum resistance force per unit root surface area is defined as the shear strength of the root-soil interface, see Equation (3).

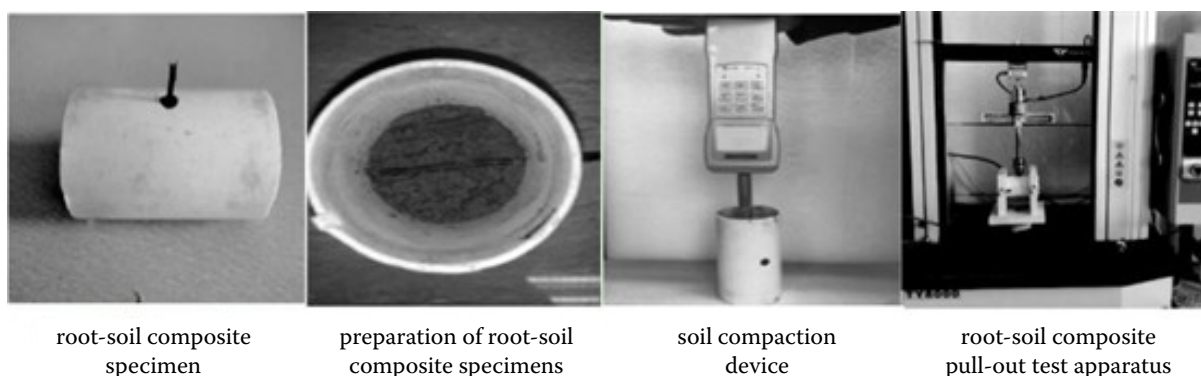


Figure 2. Preparation of root-soil composite specimens and processes of soil compaction and pull-out testing

$$\tau\pi dl - F = 0 \quad (3)$$

where:

- $\tau$  – pull-out shear stress at the root-soil interface (kPa);
- $F$  – maximum pull-out force when the root is extracted (N);
- $d$  – average diameter of the root (cm);
- $l$  – length of the root embedded in the soil (cm).

## RESULTS

This study measured the single-root tensile resistance of five plant species – alfalfa (*Medicago sativa*), peashrub (*Caragana korshinskii*), Mongolian sweetvetch (*Corethrodendron liguosum*), sea-buckthorn (*Hippophae rhamnoides*), and erect milkvetch (*Astragalus adsurgens*) – in both loessial soil and aeolian sandy soil, under soil moisture conditions ranging from 4.6% to 20.6%. The results demonstrated that single-root tensile resistance was significantly influenced by both soil type and moisture content.

**Tensile resistance of single roots of five plant species versus soil moisture under two soil types.** Figure 3 illustrates the variation in single-root tensile resistance with soil moisture content for five plant species in both loessial and aeolian sandy soil. As shown, the tensile resistance in both soil types initially increased and then decreased with rising moisture content. Curve regression analysis was performed on this relationship for all five species in both soils. The corresponding fitting equations and coefficients of determination ( $R^2$ ) are presented in Figure 3. The relationship was best described by a polynomial function, conforming to the model  $Y = ax^2 + bx + c$ , with all multiple correlation coefficients exceeding 0.5. For all five species, the single-root tensile resistance peaked at a soil moisture content of 8.6% in both soil types, after which it gradually decreased with further increases in moisture. This indicates the existence of an optimal moisture content for the mobilisation of root-soil interface friction. As shown in Figure 3, statistical analysis revealed significant differences ( $\alpha = 0.05$ ) in single-root tensile resistance across different moisture levels for all five plants in both loessial and aeolian sandy soil, demonstrating a pronounced influence of soil moisture content on this mechanical property.

In loessial soil, the tensile resistance ranges for each species were as follows: *Medicago sativa* (0.17–0.83 N), *Caragana Korshinskii* (0.13–0.76 N), *Hedysarum mongolicum* (0.13–0.59 N), *Hippophae rhamnoides* (0.14–0.95 N), and *Astragalus adsurgens* (0.18–0.81 N). The corresponding ranges in aeolian sandy soil were: *Medicago sativa* (0.10–0.24 N), *Caragana Korshinskii* (0.02–0.14 N), *Hedysarum mongolicum* (0.05–0.26 N), *Hippophae rhamnoides* (0.12–0.22 N), and *Astragalus adsurgens* (0.06–0.20 N). Overall, the mean tensile resistance in loessial soil was significantly higher than that in aeolian sandy soil ( $P < 0.05$ ). The ranking of tensile resistance among species in loessial soil varied with moisture content; however, sea-buckthorn, alfalfa, and erect milkvetch generally exhibited higher values than peashrub and Mongolian sweetvetch. In contrast, the ranking in aeolian sandy soil showed no consistent pattern across different moisture levels. These results indicate that, from the perspective of root-soil interfacial friction characteristics, the tested plants contribute more effectively to enhancing the mechanical stability of the surface soil in loessial soil than in aeolian sandy soil.

Based on the findings above, the ranking of the five plant species by their single-root tensile resistance changes with varying soil moisture levels under the same soil type. In natural environments, soil moisture is in a constant state of spatiotemporal fluctuation due to meteorological factors such as air temperature, solar radiation, and wind, as well as processes like plant transpiration and soil evaporation. Therefore, from the perspective of root-soil interfacial friction characteristics alone, this study's results also indirectly confirm that in slope management engineering, the use of mixed forest-grass measures with different tree species provides superior stability in root reinforcement mechanical performance under changing soil moisture conditions – and thus enhances surface soil mechanical stability more effectively – than monocultures composed of a single species.

**Single-root pull-out shear strength of five plant species versus soil moisture under two soil types.** Figure 4 shows the variation in single-root pull-out shear strength with soil moisture content for the five plant species in both loessial soil and aeolian sandy soil. As illustrated, the shear strength in both soils initially increased and then decreased with rising moisture content,

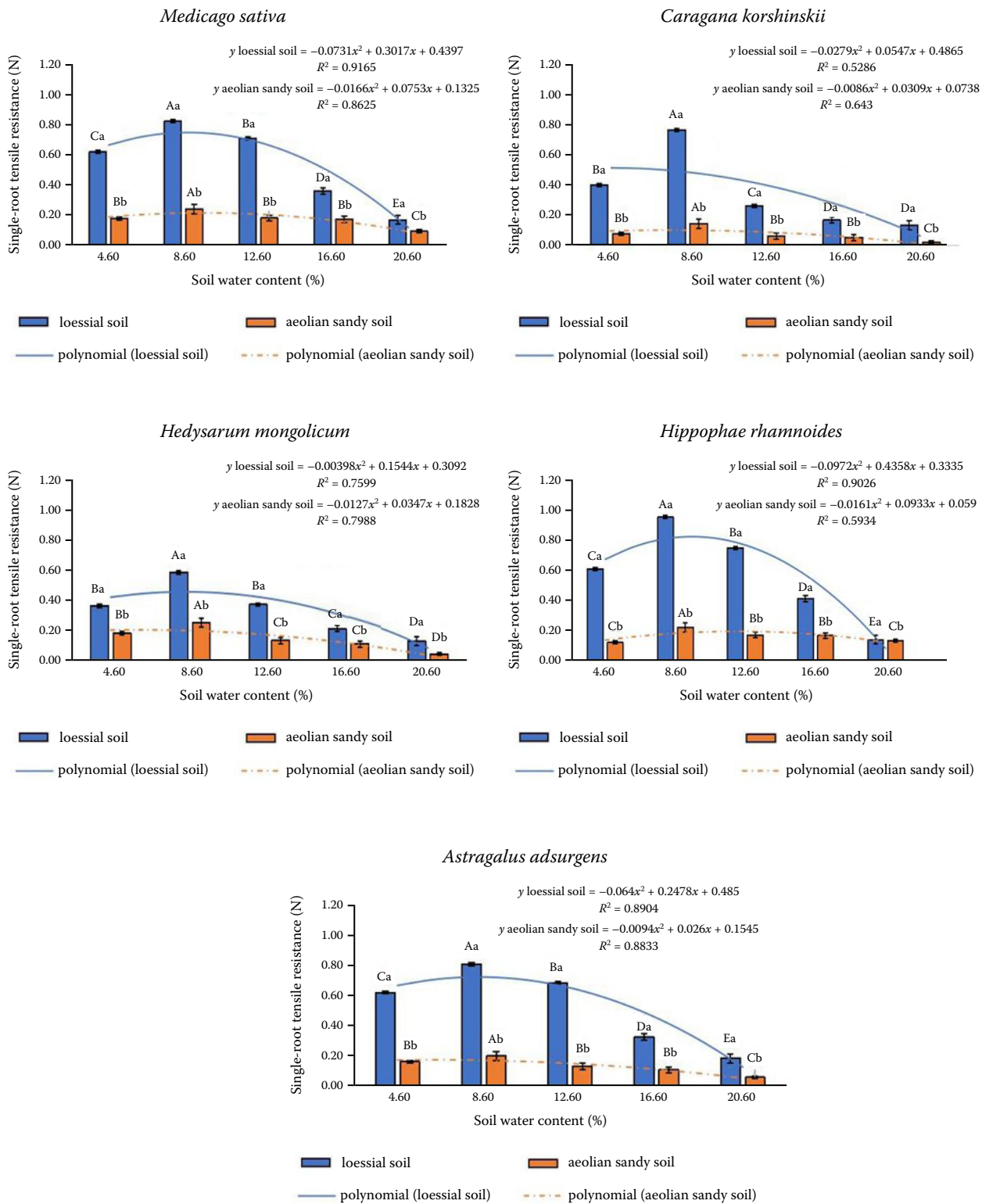


Figure 3. Variations in root-soil interfacial pull-out resistance of five plant species under five soil moisture gradients in two soil types

Capital letters indicate the results of significance tests for differences in single-root pull-out resistance under different moisture contents for the same plant species and soil type, while lowercase letters indicate the results of significance tests for differences in single-root pull-out resistance under different soil types at the same moisture content for the same plant species; the same letters denote no significant difference, whereas different letters indicate significant differences ( $\alpha = 0.05$ )

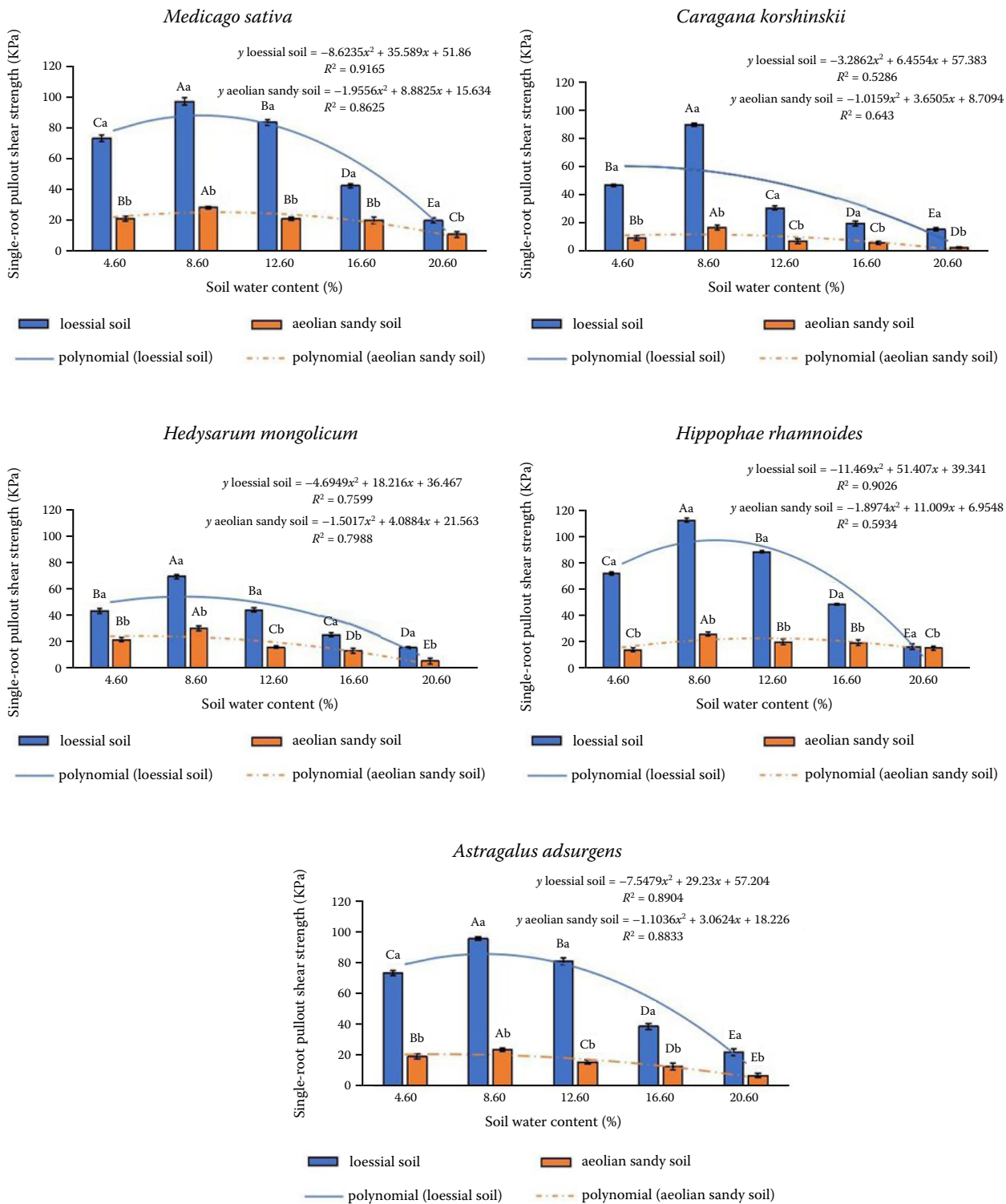


Figure 4. Variations in root-soil interfacial pull-out resistance of five plant species across five soil moisture gradients in two soil types

Capital letters indicate the results of significance tests for differences in single-root pull-out frictional strength under different moisture contents for the same plant species and soil type, while lowercase letters indicate the results of significance tests for differences in single-root pull-out frictional strength under different soil types at the same moisture content for the same plant species; identical letters denote no significant difference, whereas different letters indicate significant differences ( $\alpha = 0.05$ )

peaking at 8.6% moisture before gradually declining thereafter. The relationship was best described by a polynomial function (Figure 4), conforming to the model  $Y = ax^2 + bx + c$ , with all multiple correlation coefficients exceeding 0.5. This trend is consistent with the pattern observed for single-root tensile resistance in response to changing soil moisture.

In summary, a comprehensive comparison reveals that the single-root pull-out shear strength of the five plant species differed significantly ( $\alpha = 0.05$ ) across different soil moisture levels in both loessial soil and aeolian sandy soil. The strength peaked at a moisture content of 8.6% in both soils, indicating a pronounced influence of soil moisture on this property. In loessial soil, the mean single-root pull-out shear strength of the five species ranked as follows: *Hippophae rhamnoides* ( $67.40 \pm 8.25$  KPa) > *Medicago sativa* ( $63.77 \pm 6.48$  KPa) > *Astragalus adsurgens* ( $61.87 \pm 5.94$  KPa) > *Caragana Korshinskii* ( $40.60 \pm 4.25$  KPa) > *Hedysarum mongolicum* ( $39.47 \pm 4.37$  KPa), with significant differences among them ( $P < 0.05$ ). In aeolian sandy soil, the ranking was: *Medicago sativa* ( $20.77 \pm 3.05$  KPa) > *Hippophae rhamnoides* ( $19.11 \pm 2.48$  KPa) > *Hedysarum mongolicum* ( $17.31 \pm 1.85$  KPa) > *Astragalus adsurgens* ( $15.27 \pm 1.88$  KPa) > *Caragana Korshinskii* ( $8.49 \pm 1.15$  KPa), also with significant differences ( $P < 0.05$ ). This disparity was substantial. For instance, at the 4.6% moisture level, the strength values in loessial soil were 49.80% (*Hedysarum mongolicum*) to 80.25% (*Hippophae rhamnoides*) higher than those in aeolian sandy soil.

Based on the comprehensive findings presented above, and solely from the perspective of root-soil interfacial friction characteristics, the ability of plant roots to reinforce soil, conserve water, and enhance the mechanical stability of surface soil is not only influenced by plant species but also varies with soil type. Furthermore, when comparing the two soil types, the loessial soil environment is more conducive to the expression of root-soil interfacial friction. This study also demonstrates that even for the same plant species in the same soil type, the soil-reinforcing effect of the roots is not constant; rather, it changes with variations in soil moisture content.

**Comprehensive influence of various factors on root-soil frictional performance.** Figure 5 presents the results of the Redundancy Analysis (RDA) (Ma'ruf 2012; Guo et al. 2021) examining the root-soil frictional characteristics of the five plant species and various influencing factors. The ordination diagram reveals the intrinsic relationships among the variables through two primary axes. Axis 1, which accounts for 84.64% of the explained variance, serves as the primary dimension characterising these variable relationships. Axis 2 contributes an additional 6.29% to the explained variance. Cumulatively, the two axes explain 90.93% of the total variance, indicating that the RDA ordination effectively captures the overall relationship between plant root-soil frictional characteristics and the environmental factors. The distribution of variable factors shows that mechanical indicators, such as single-root pull-out shear strength and single-root tensile resistance, exhibit a signifi-

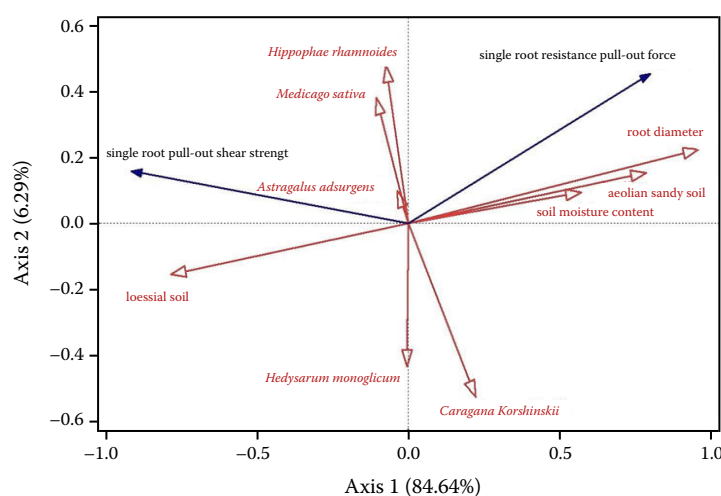


Figure 5. Analysis of root-soil friction characteristics and influencing factors for five plant species

cant positive correlation with Axis 1. This suggests that these mechanical properties are primarily driven by the first principal axis. Factors like root diameter and soil moisture content also show a positive correlation with Axis 1, indicating that root morphological traits and soil moisture conditions significantly influence the pull-out mechanical performance of single roots. The aeolian sandy soil factor is located in the negative region of the ordination plot, implying potential differences in how this soil type affects root reinforcement capacity compared to others. The spatial distribution of each plant species within the ordination diagram reflects their respective response strategies of root pull-out resistance characteristics to environmental factors. Sea-buckthorn and alfalfa are clustered in the positive axis region, indicating their superior single-root pull-out mechanical performance. The distribution patterns of erect milkvetch, Mongolian sweetvetch, and peashrub suggest that the pull-out resistance characteristics of these species are associated with specific environmental factors in distinct ways.

From a mechanistic perspective, these RDA ordination results elucidate the intrinsic relationships between the single-root pull-out mechanical properties of plants and environmental factors, thereby providing a theoretical basis for selecting suitable sand-stabilising plant species for different site conditions.

## DISCUSSION

This study investigates five plant species in loessial soil and aeolian sandy soil, with soil moisture content ranging from 4.6% to 20.6%. As soil moisture content increases, the single root tensile resistance and pull-out shear strength initially increase and then decrease, following the model  $Y = ax^2 + bx + c$  (with multiple correlation coefficients all  $> 0.5$ ). Zhou et al. (2011) found that under four different soil moisture levels, the values were higher than those of pure soil. The cohesion strength of the two plant species showed trends similar to those of pure soil, both related to residual strength. When soil moisture content increases, the internal friction angle decreases, a conclusion also supported by the findings of this study. The analysis suggests (Genet et al. 2005) that when capillary water is present at the root-soil interface, the wetting effect on the root-soil surface

causes the capillary water meniscus to curve inward. At the water-air interface, surface tension is generated along the tangential direction of the curved surface, pointing inward. This tension creates capillary pressure at the root-soil interface, enhancing the cohesion between roots and soil. This cohesion initially increases (Waldron, Dakesian 1981) and then decreases (Schwarz et al. 2011) with rising soil moisture content, leading to a similar trend in the interaction forces between roots and soil. As soil moisture content continues to increase, soil saturation rises, and the increase in water molecules enhances the pore water pressure between soil particles, increasing matric suction (Watson et al. 2000). The strong and weak bound water in the soil gradually reach an equilibrium state, and the root-soil interface becomes fully bonded. At this point, soil cohesion reaches its maximum, and the friction at the root-soil interface peaks. With further increases in soil moisture content, soil saturation continues to rise, reducing cohesion and matric suction between soil particles. The thickening of the weak bound water film weakens the molecular attraction between soil particles, and the interlocking between roots and soil diminishes, resulting in a decrease in friction between them (Xiao 2016). Existing research indicates that single root tensile resistance and tensile strength are closely related to root diameter. Single root tensile resistance increases as a power function with increasing root diameter (Norris 2005), while single root tensile strength decreases as a power function with increasing root diameter (Zhang et al. 2021). Moreover, significant differences in single-root tensile resistance and tensile strength are observed among different plant species, which contrasts with the trends observed in this study.

In soil, particles are bonded together through various attractive forces. These forces are primarily physical attractions such as van der Waals forces, Coulomb forces, and the surface tension of water films, which characterise soil shear strength, erosion resistance, and disintegration properties (Gao et al. 2023). For the five plant species, at the same moisture content, the values of single root tensile resistance and pull-out shear strength in loessial soil were consistently greater than those in aeolian sandy soil. Similar results have been obtained in other related studies (Li et al. 2020), where researchers consistently found that herbaceous plant roots can enhance soil shear strength.

Analysis of the reasons reveals that the fine particle fraction (< 0.075 mm) in loessial soil accounts for 54.83%, significantly higher than the 0.1% in aeolian sandy soil. Finer soil particles increase compactness, leading to greater contact pressure between roots and the soil matrix, thereby enhancing static friction (Mao et al. 2012). The lower single root tensile resistance in aeolian sandy soil compared to loessial soil may be attributed to the coarse texture, poor water retention capacity, and weak cohesion between soil particles in aeolian sandy soil. In contrast, the finer particles of loessial soil provide a larger specific surface area, allowing for tighter contact with root surfaces and enhanced interlocking between particles, which increases the frictional resistance at the root-soil interface. Meanwhile, the coarse and loose structure of aeolian sandy soil makes it prone to particle slippage during pull-out tests, resulting in lower pull-out shear strength. Additionally, the higher clay content in loessial soil may contribute to weak cohesion at the root-soil interface, further improving shear resistance (Norris et al. 2008).

Under the same soil type and moisture content, the frictional characteristics at the root-soil interface vary among plant species. For example, sea buckthorn exhibits the highest single root pull-out shear strength (112.11 kPa) in loessial soil, whereas the values for littleleaf peashrub (15.64 kPa) and Mongolian sweetvetch (15.64 kPa) are significantly lower. This discrepancy may be attributed to differences in root epidermal roughness. For instance, the high surface roughness of sea buckthorn roots enhances mechanical interlocking with soil particles, while the relatively smooth root surfaces of littleleaf peashrub result in weaker shear resistance (Wu 2013). The variability in root epidermal roughness introduces uncertainties in the random distribution of soil particles around roots and the variable bonding conditions at the root-soil interface, leading to differences in frictional characteristics. Further detailed research is necessary to determine the optimal root content and moisture content for enhancing soil shear strength across the five plant species. Subsequent studies should incorporate microscopic structural analyses, such as root epidermal roughness, to advance understanding in this area (Docker, Hubble 2008).

Based on a comprehensive analysis of the single root pull-out shear strength of five plant species and various influencing factors, redundancy

analysis (RDA) with stepwise screening indicates that 'soil type + soil moisture content' exhibits strong explanatory power for the vegetation-soil coupling system (Veylon et al. 2015). The five plant species, including sea buckthorn, demonstrate similar correlation patterns with single root pull-out shear strength in the loessial soil environment, with sea buckthorn being more significantly influenced by environmental regulation. Subsequent research could further explore the adaptive mechanisms linking plant characteristics, environmental conditions, and mechanical properties.

## CONCLUSION

Based on single root pull-out tests of five native species in central-western Inner Mongolia, this study demonstrates that both single root pull-out resistance and shear strength initially increase and then decrease with rising soil moisture, peaking at 8.6%. Soil reinforcement effectiveness ranks as: *Hippophae rhamnoides* > *Medicago sativa* > *Astragalus adsurgens* > *Caragana microphylla* > *Hedysarum mongolicum*. The shear strength is significantly higher in loessial soil than in sandy soil. Redundancy analysis confirms that soil type and moisture content are key factors driving shear strength variation, with *H. rhamnoides* showing the strongest environmental response. These findings provide a mechanical basis for selecting species for soil fixation, and future studies should focus on plant-environment-mechanics adaptation mechanisms under varying soil conditions.

## REFERENCES

- Ali N., Farshchi I., Mu'azu M.A., Rees S.W. (2012): Soil-root interaction and effects on slope stability analysis. The Electronic Journal of Geotechnical Engineering, 17: 319–328.
- Bardgett R.D., Mommer L., De Vries F.T. (2014): Going underground: Root traits as drivers of ecosystem processes. Trends in Ecology & Evolution, 29: 692–699.
- Berry S.L., Roderick M.L. (2005): Plant-water relations and the fibre saturation point. New Phytologist, 168: 25–37.
- Bordoni M., Meisina C., Vercesi A., Bischetti G.B., Chiardia E.A., Vergani C., Chersich S., Valentino R., Bittelli M., Comolli R., Persichillo M.G., Cislaghi A. (2016): Quantifying the contribution of grapevine roots to soil mechanical reinforcement in an area susceptible to shallow landslides. Soil & Tillage Research, 163: 195–206.

Campbell K.A., Hawkins C.D. (2003): Paper birch and lodgepole pine root reinforcement in coarse-, medium-, and fine-textured soils. *Canadian Journal of Forest Research*, 33: 1580–1586.

Docker B.B., Hubble T.C.T. (2008): Quantifying root reinforcement of river bank soils by four Australian tree species. *Geomorphology*, 100: 401–418.

Fan C.C., Chen Y.W. (2010): The effect of root system architecture on providing shearing resistance to root-permeated soils. *Ecological Engineering*, 36: 813–826.

Fan C.C., Lu J.Z., Chen H.H. (2021): The pullout resistance of plant roots in the field at different soil water conditions and root geometries. *Catena*, 207: 105593.

Fang X., Wang Z., Shen C., Chen C., Yao Z. (2024): Study on the pullout bearing characteristics of root piles in coral sand foundations under different water content states. *Applied Ocean Research*, 146: 103962.

Flores-Rentería D., Yuste C.J., Valladares F., Rincón A. (2018): Soil legacies determine the resistance of an experimental plant-soil system to drought. *Catena*, 166: 271–278.

Gao Q.F., Yu H., Zeng L., Zhang R., Zhang Y.H. (2023): Roles of vetiver roots in desiccation cracking and tensile strengths of near-surface lateritic soil. *Catena*, 226: 107068.

Genet M., Stokes A., Salin F., Mickovski S.B., Fourcaud T., Du-mail J.F., Van Beek R. (2005): The influence of cellulose content on tensile strength in tree roots. *Plant and Soil*, 278: 1–9.

Gonzalez-Ollauri A., Mickovski S.B. (2017): Plant-soil reinforcement response under different soil hydrological regimes. *Geoderma*, 285: 141–150.

Guo N., Li L., Cui J., Cai B. (2021): Effects of *Funneliformis mosseae* on the fungal community in and soil properties of a continuously cropped soybean system. *Applied Soil Ecology*, 164: 103930.

Hales T.C., Cole-Hawthorne C., Lovell L., Evans S.L. (2013): Assessing the accuracy of simple field based root strength measurements. *Plant and Soil*, 372: 553–565.

Ji X.D., Cong X., Dai X.Q., Zhang A., Chen L.H. (2018): Studying the mechanical properties of the soil-root interface using the pullout test method. *Journal of Mountain Science*, 15: 882–893.

Li M., Wang X., Zhang C. (2020): A comparative study on root tensile strength and chemical composition of five shrubs and herbs for slope protection in arid regions. *Catena*, 194: 104681.

Mao Z., Saint-André L., Genet M., Mine F.X., Jourdan C., Rey H., Courbaud B., Stokes A. (2012): Engineering ecological protection against landslides in diverse mountain forests: Choosing cohesion models. *Ecological Engineering*, 45: 55–69.

Ma'ruf F.M. (2012): Shear strength of *Apus* bamboo root reinforced soil. *Ecological Engineering*, 41: 84–86.

Noorasyikin M.N., Zainab M., Derahman A., Dan M.M., Madun A., Yusof Z.M., Pakir F. (2022): Mechanical properties of Bermuda grass roots towards sandy and clay soil for slope reinforcement. *Physics and Chemistry of the Earth*, 128: 103261.

Norris E.J. (2005): Root reinforcement by hawthorn and oak roots on a highway cut-slope in Southern England. *Plant and Soil*, 278: 43–53.

Norris J.E., Di Iorio A., Stokes A., Nicoll B.C., Achim A. (2008): Species selection for soil reinforcement and protection. In: Norris J.E., Stokes A., Mickovski S.B., Cammeraat E., van Beek R., Nicoll B.C., Achim A. (eds): *Slope Stability and Erosion Control: Ecotechnological Solutions*. Dordrecht, Springer: 167–210.

Schwarz M., Cohen D., Or D. (2010). Root-soil mechanical interactions during pullout and failure of root bundles. *Journal of Geophysical Research*, 115: 701–719.

Schwarz M., Cohen D., Or D. (2011): Pullout tests of root analogs and natural root bundles in soil: Experiments and modeling. *Journal of Geophysical Research: Earth Surface*, 116: 167–177.

Tosi M. (2007): Root tensile strength relationships and their slope stability implications of three shrub species in the Northern Apennines (Italy). *Geomorphology*, 87: 268–283.

Veylon G., Ghoshem M., Stokes A., Bernard A. (2015): Quantification of mechanical and hydric components of soil reinforcement by plant roots. *Canadian Geotechnical Journal*, 52: 1839–1849.

Waldron L.J., Dakessian S. (1981): Soil reinforcement by roots: Calculation of increased soil shear resistance from root properties. *Soil Science*, 132: 427–435.

Watson A., Phillips C., Marden M. (2000): Root strength, growth, and rates of decay: Root reinforcement changes of two tree species and their contribution to slope stability. In: Stokes A. (ed.): *The Supporting Roots of Trees and Woody Plants: Form, Function and Physiology*. Dordrecht, Springer Netherlands: 41–49.

Wu T.H. (2013): Root reinforcement of soil: review of analytical models, test results, and applications to design. *Canadian Geotechnical Journal*, 50: 259–274.

Xiao Y. (2016): Discussion of 'Dilatancy and friction angles based on *in situ* soil conditions' by Ozer Cinicioglu and Arshiya Abadkon. *Journal of Geotechnical and Geoenvironmental Engineering*, 142: 07016009.

Xing S., Zhang G., Zhu P., Wang L., Wang Z., Wang C. (2023): Variation in shear strength of soil-root system under five typical land use types on the Loess Plateau of China. *Catena*, 222: 106883.

Zhang C.B., Liu Y.T., Li D.R., Jiang J. (2020): Influence of soil moisture content on pullout properties of *Hippophae rhamnoides* Linn. Roots. *Journal of Mountain Science*, 17: 2816–2826.

<https://doi.org/10.17221/95/2025-JFS>

Zhang C., Liu B., Li M. (2021): Root morphological traits and biomechanical properties of *Medicago sativa* under different soil types and their correlations with pull-out resistance. *Soil & Tillage Research*, 213: 105147.

Zhang S., Ma J., Liu S., Zhang L., Li Z., She F., Ding J., Li P., Tian C. (2025): Corrigendum to 'Effects of herbaceous plant roots on tensile strength of root-soil composite in loess hilly region'. *Catena*, 260: 109499.

Zhou D.D., Liu J., Yao X.J., Zhang X., Hu N. (2011): Effects of soil moisture content on the residual strength of two plants root-soil composites. *Advanced Materials Research*, 1328: 160–164.

Received: December 11, 2025

Accepted: January 19, 2026

Published online: January 30, 2026